

# Artificial Intelligence-Driven Optimization of a 34 GHz Compact Arrow-Shaped Microstrip Antenna for 5G Wireless Applications

Jawdat S. Alkasassbeh<sup>1\*</sup>, Farouq Mohammad Al-Taweel<sup>1</sup>, Majed O. Dwairi<sup>1</sup>, Aws Al-Qaisi<sup>2</sup>, and Maen Takruri<sup>2</sup>

<sup>1</sup>Department of Electrical Engineering, Faculty of Engineering Technology, Al-Balqa Applied University, Amman, Jordan

Jawdat1983@bau.edu.jo ; dr\_farouq@bau.edu.jo; majeddw@bau.edu.jo

<sup>2</sup>College of Engineering and Technology, American University of the Middle East, Egaila 54200, Kuwait

Aws.Al-Qaisi@aum.edu.kw ; maen.takruri@aum.edu.kw

## Abstract

*This paper presents a compact millimeter-wave antenna for 5G applications, featuring a partial ground plane and an arrow-shaped patch. The patch is an equilateral triangle with a side length of 2.4 mm and a 0.3 mm hollow triangular slot, implemented on a Rogers RT/Duroid 5880 substrate measuring  $10.2 \times 11.8 \times 0.254$  mm<sup>3</sup>. The antenna operates across 30.6–36.6 GHz, achieving a 6 GHz bandwidth and a resonant frequency of 34 GHz. Optimization yielded a maximum gain of 4.2 dB and a return loss of -29.82 dB at the resonant frequency. The design process employed CST Studio Suite 2018, with performance enhancements achieved by introducing slots and triangular cuts in the partial ground plane. This antenna's compact size, wide bandwidth, and stable gain make it highly suitable for 5G applications such as high-speed data transfer, low-latency communications, and enhanced mobile broadband. Its design also ensures easy integration into portable 5G devices, base stations, and other compact communication systems, offering a practical and efficient solution for next-generation wireless networks.*

**Keywords:** Ultrawideband ;5G; Microstrip antenna; Return loss; mmWave

## 1 Introduction

The fast development of wireless communication systems requires systems which deliver fast data transfer with minimal delay and maximum reliability. The fifth-generation (5G) network infrastructure depends on millimeter wave (mmWave) frequencies because they offer broad frequency ranges and fast data transfer rates. The compact design of microstrip antennas has become popular for mmWave applications because they offer small size and low height and light weight and simple integration

with which include split ground planes and MIMO systems and advanced patch designs. A dual-band mmWave antenna printed circuit boards. The development of microstrip antennas requires significant improvement to fulfill 5G network requirements operating at 28 and 38 GHz frequencies has been developed to achieve 7.4 dB gain and 2.55 GHz bandwidth [1]. The development of a dual-band patch antenna for 38 and 60 GHz applications resulted in a 6.5 dB gain which shows its potential for mobile phone integration [2]. The research focuses on developing antennas for military Ka-band applications through the design of a specific antenna which achieves 5.34 GHz bandwidth and 33.83 GHz resonant frequency [3]. The design of a circularly polarized antenna for 5G networks has been proposed to achieve 4.01 dB gain at its specific resonant frequency [4]. The development of small devices which operate across broad frequency ranges at millimeter wave frequencies faces major obstacles despite recent breakthroughs in this field.

The research presents a compact arrow-shaped microstrip antenna which operates at 34 GHz for 5G applications through the combination of a partial ground plane and a hollowed triangular patch structure to achieve optimal performance between size and bandwidth and gain.. Performance gains are obtained by thorough parametric optimization and analytical modeling. High-speed data transmission and low-latency communication are the key focal points for the advancement of antenna technologies in modern wireless systems. Microstrip antennas play a very important role in mmWave applications for 5G networks due to their compact size, low profile, lightweight design, and easy integration with circuit boards to perform an enhancement through achieving bandwidth improvement [5-7] and the integration of MIMO systems [8]. The millimeter wave bands will proffer better capacity and throughput compared with the conventional frequency bands of wireless systems-as it goes-driven by proliferating user devices demanding data. In this paper, different aspects of 5G antenna design are discussed, showing great emphasis on their shapes and unique configurations to get a set of new bands and resonant frequencies that optimally perform for 5G applications. Different geometries of microstrip patch antennas were used and considered for mmWave and UWB applications in several works [9-11] in single and MIMO configurations for the purpose of enhancing gain or bandwidth. For instance, a novel QSDGS was proposed in [12] that allows for the possibility of designing a wideband microstrip antenna suitable for 5G use cases. Similarly, [13] designed a 2×2 MIMO antenna and planar dual-frequency mmWave printed monopole antenna with a radiating element of a rectangular-shaped monopole operating at 28 GHz and 38 GHz, respectively. In [14], a compact dual-frequency microstrip patch antenna was described with electromagnetically coupled dual patches. The said antenna offered the dual-band operation at 38 GHz and 60 GHz. This antenna implemented the capacitive and inductive coupling to ensure different radiations for both lower-band and higher-band operation. a circularly polarized antenna with a hook-shaped aperture that exhibits a gain of 4.01 dB at 3.47 GHz is presented in [15] . In [16], an octagonal patch antenna with impedance matching and resonant frequency adjustments was proposed to operate within a bandwidth of 5.34 GHz over the frequency range of 32.16-37.5 GHz. In [17, 29], a multiband design was developed with three resonant frequencies. Besides, microstrip antennas have been explored for Wi-Fi and C-band applications in the super-high frequency range, showing their versatility across diverse wireless communication domains. Furthermore, a microstrip antennas for Wi-Fi and C-band applications in the super-high frequency region. with continuous evolution of 5G technology necessitates novel solutions to the issues of high-speed, low-latency, and dependable wireless

communication [19-23]. Millimeter-wave (mmWave) frequencies are critical for satisfying these requirements, and microstrip antennas have emerged as a potential technology due to their compact size, low profile, and ease of integration. This article provides a novel antenna design suited for 34 GHz applications that focuses on important performance indicators as bandwidth, gain, and integration capabilities. The main contributions of this work are stated below:

1. This study presents a compact arrow-shaped microstrip antenna with a hollow triangular patch and a partial ground plane, optimized for 5G applications at 34 GHz that achieves a bandwidth of 6 GHz (30.6–36.6 GHz) with a maximum gain of 4.2 dB, and a return loss of -29.82 dB which is ensuring high performance and stable operation.
2. It combines a low attenuation with a compact size ( $10.2 \times 11.8 \times 0.254 \text{ mm}^3$ ) facilitating seamless integration into portable 5G devices by utilizing an RT/Duroid substrate.
3. It contributes to transfer a high-speed data with low-latency broadband communications system that offering a practical and efficient solution for next-generation wireless networks.

The remaining sections of this paper are organized as follows: Section 2 outlines the antenna design, Section 3 presents the results and discussion, and Section 4 concludes the study.

## 2 Antenna Design

A compact and effective antenna is designed for 5G applications operating at 34 GHz. For this design, critical parameter calculations, optimization, and simulation were done based on using the Rogers RT5880 substrate because of its minimum attenuation at high frequencies and low dielectric constant. Some of the key characteristics of this substrate are a dielectric constant ( $\epsilon_r$ ) of 2.2, a thickness ( $T_s$ ) of 0.254 mm, and a loss tangent as low as 0.0009. In order to guarantee compatibility with portable devices, the maximum dimensions of the antenna were limited to  $12 \times 12 \text{ mm}$ . By taking advantage of the excellent high-frequency performance of Rogers RT5880, the proposed antenna operates at 34 GHz. The substrate's low dielectric constant, minimal attenuation, and physical properties in terms of thickness (0.254 mm), loss tangent (0.0009), and dielectric constant (2.2) substantiate the design goals. Numerical optimization led to the determination of the final dimensions of the antenna:  $10.2 \times 11.8 \times 0.254 \text{ mm}^3$ . A partial ground plane was used in this antenna design, with optimized slots included in it for the target resonant frequency.

Fig. 1(a) and Fig. 1(b) are the proposed arrow-shaped antenna viewed from the front and rear sides, respectively. The antenna is excited through a  $50 \Omega$  microstrip inset feed and can support an operational bandwidth ranging from 30 to 36.6 GHz. The design, simulation, optimization, and testing of the proposed design were performed in CST Studio Suite 2018. Calculations of the design parameters were carried out using pre-defined equations available in [8,11-12]. Accordingly, the patch width was calculated using Equation (1).

$$W_p = \frac{c}{2f_r} \sqrt{\frac{2}{\epsilon_r + 1}} \quad (1)$$

By substitution, we calculated  $W_p = 3.89 \text{ mm}$ . Additionally, the effective dielectric constant can be determined using Equation (2).

$$\epsilon_{eff} = \frac{\epsilon_r + 2}{2} + \frac{\epsilon_r - 1}{2 \sqrt{1 + 12 \frac{h_s}{W_p}}} \quad (2)$$

By successive substitution  $\epsilon_{\text{reff}} = 2.05$ . The extended incremental length of the patch  $\Delta L$  is, using the following Equation (3)

Through successive substitution, the effective dielectric constant ( $\epsilon_{\text{reff}}$ ) was calculated to be 2.05. The extended incremental length of the patch ( $\Delta L$ ) is determined using Equation (3).

$$\Delta L = \frac{0.412 \times h_s (\epsilon_{\text{reff}} + 0.3) \left( \frac{W_p}{h_s} + 0.264 \right)}{(\epsilon_{\text{reff}} - 0.258) \left( \frac{W_p}{h_s} + 0.8 \right)} \quad (3)$$

In sequence, the extended incremental length ( $\Delta L$ ) is calculated to be 0.132 mm. Using Equation (4), the patch's effective length can now be determined as follows.

$$L_{\text{eff}} = \frac{c}{2f_r \sqrt{\epsilon_{\text{reff}}}} \quad (4)$$

In succession, the effective length ( $L_{\text{eff}}$ ) is calculated to be 3.08 mm. Finally, the actual length of the patch ( $L_p$ ) can be determined using Equation (5).

$$L_p = L_{\text{eff}} - 2 \Delta L = 3.08 - 2 * 0.132 = 2.816 \text{ mm} \quad (5)$$

The antenna parameters are calculated to ensure resonance at 34 GHz. The chosen patch geometry is an equilateral triangle with a side length ( $W_p$ ) of 2.4 mm and a patch length ( $L_p$ ) of 2.08 mm. This antenna should be optimized to reach an exact resonance frequency of 34 GHz. The simulation process involves four different models, which are described in the next section. The algorithm framework below shows the step-by-step methodology to design the antenna through simulation and optimization steps for the Arrow-Shaped Microstrip Antenna Design for 5G Applications.

#### Input:

*Parameter bounds:*

- Patch length ( $L_p$ ): [2.0 mm, 3.0 mm]
- Slot thickness ( $T_s$ ): [0.1 mm, 0.5 mm]
- Ground cut dimension ( $G_c$ ): [1.0 mm, 2.0 mm]

*Target performance metrics:*

- Target return loss ( $RL_{\text{target}}$ ): -29.82 dB
- Target gain ( $G_{\text{target}}$ ): 4.2 dB
- Bandwidth range ( $BW_{\text{range}}$ ): [30.6 GHz, 36.6 GHz]

*Optimization hyperparameters:*

- Population size ( $pop\_size$ ), Number of generations ( $gen\_max$ ), Mutation rate ( $mutation\_rate$ )

#### Define Objective Function:

- Compute performance metrics based on the design: return loss (RL), gain (G), and bandwidth (BW).
- Combine objectives into a single cost function using weights:

$$F = w_1 \cdot |RL - RL_{\text{target}}| + w_1 \cdot \max(0, G_{\text{target}} - G) + w_3 \cdot \text{penalty for BW out of range}$$

#### Output:

- Optimized design parameters:  $L_p, T_s, G_c$
- Select the design with the lowest cost  $F$ .
- Validate through additional simulations.

**Key Steps**

1. Start with a diverse set of designs as initialization state
2. Use CST Studio (or equivalent) to simulate antenna performance and compute fitness based on return loss, gain, and bandwidth which leads to make the Fitness Evaluation.
3. Use evolutionary principles to explore and refine designs to do the Selection, Crossover and Mutation stages
4. Stop after a fixed number of generations or when the solution is stable termination stage.

---

**Algorithm 1: Min-Max Optimization Algorithm for Arrow-Shaped Microstrip Antenna Design**


---

1. **Initialize** a random population of design parameters within bounds for each individual in the population:
  - 1.1 Randomly generate  $L_p \in [2.0 \text{ mm}, 3.0 \text{ mm}]$
  - 1.2 Randomly generate  $T_s \in [0.1 \text{ mm}, 0.5 \text{ mm}]$
  - 1.3 Randomly generate  $G_c \in [1.0 \text{ mm}, 2.0 \text{ mm}]$
2. **Evaluate** fitness for each individual in the population for each individual ( $L_p$ ,  $T_s$ ,  $G_c$ ):
  - 2.1 Simulate the antenna design using CST Studio or equivalent.
  - 2.2 Measure return loss (RL), gain (G), and bandwidth (BW).
  - 2.3 Compute penalties:
 
$$RL\_penalty = |RL - RL\_target|$$

$$G\_penalty = \max(0, G\_target - G)$$

$$BW\_penalty = 0 \text{ if } BW\_range[0] \leq BW \leq BW\_range[1], \text{ else } 10$$
  - 2.4 Calculate fitness score:
 
$$Fitness = W\_RL * RL\_penalty + W\_G * G\_penalty + W\_BW * BW\_penalty$$
3. **Sort** the population by fitness scores (lower is better).
4. **Select** the top 50% of the population as elites.
5. **Generate** a new population:
  - 5.1 Crossover:
 

For each pair of elites, generate a child by averaging parameters:

$$Child\_param = (Parent1\_param + Parent2\_param) / 2$$
  - 5.2 Mutation:
 

For each child parameter, apply random perturbation:

$$Child\_param = Child\_param + \text{random}(-mutation\_rate, mutation\_rate)$$
6. **Replace** the old population with the new population.
7. **Repeat** steps 2–6 for  $gen\_max$  generations or until convergence criteria are met.
8. **Output** the best individual in the final population as the optimized design:
  - 8.1 Optimized parameters:  $L_p$ ,  $T_s$ ,  $G_c$
  - 8.2 Performance metrics: RL, G, BW

---

**End**


---

The performance metrics of the arrow-shaped 34-GHz microstrip antenna for 5G applications, such as return loss, gain, and bandwidth, are improved using a Min-Max Optimization Algorithm. The algorithm starts with random design parameters, which are updated iteratively by simulation-based fitness evaluation, selection of the best designs, and evolutionary operations like crossover and mutation. Some of the major developments are a hollow triangular patch with a slotted partial ground plane, which has resulted in an antenna operating at a resonance frequency of 34 GHz, return loss of -29.82 dB, gain of 4.2 dB, and bandwidth of 6 GHz (30.6-36.6 GHz). This is compact and quite an efficient design for fast data transmission and can be easily integrated with 5G devices.

### 3 Results and Discussion

#### 3.1 Overview of Design Methodology

The next section of the paper describes the complete development cycle that leads to performance evaluation for the proposed antenna design. Therefore, a systematic optimization process was able to achieve all the necessary criteria of 5G applications such as return loss, resonant frequency, and bandwidth and gain. The subsequent subsections will explain each design iteration through their corresponding modifications and resulting improvements in performance.

##### I. Initial Design and Challenges

This antenna design used an equilateral triangular patch with a uniform partial ground plane. From the model parameters in Table 1, one can see that the side length was 2.4 mm while the dimensions for the substrate were  $10.2 \times 11.8 \text{ mm}^2$ . The first model design is presented in Fig. 1(a) from its front and back sides. Simulation results in Fig. 2 indicated that this model failed to achieve the required return loss performance since it did not exhibit any resonance within the operating frequency. It was then evident that structural changes needed to be made in order to enhance antenna performance.

Table 1. Antenna parameters

<i>Parameters</i>	Calculated mm	Optimized mm
$W_s, W_g$	12	11.8
$L_s$	12	10.2
$W_p = a$	3.89	2.4
$L_p$	2.816	2.08
$h_s$	-	0.254
$t_p = t_g$	-	0.009
$L_f$	-	6.95
$W_f$	-	1.2
$L_g$	-	5
Thickness of the triangular ring	b	0.3
	c	2
	d	1.5
Ground cut	e	0.42
	f	2.5
	g	3.5

##### II. First Iterative Improvement: Slot Integration

To address the shortcomings of the first model, a rectangular slot was introduced in the upper center of the partial ground plane, as shown in Fig. 1(b). Additionally, the slot aims improving the antenna's impedance matching and enhance resonance. Simulation results in Fig. 2 demonstrated a resonant frequency at 37.4 GHz with a return loss of -26.5 dB and an operating bandwidth of 33.36–40.8 GHz. While the modifications yielded better performance, the resonant frequency deviated from the target 34 GHz.

##### III. Further Optimization: Triangular Cuts

The third iteration brought triangular cuts to the upper edges of the partial ground plane which appears in Fig. 1(c). The design modification aimed to achieve better resonant frequency performance and improved return loss optimization of the antenna. The simulation results in Fig. 2 showed a resonant frequency of 34.25 GHz with a return loss of -24.44 dB and an operational bandwidth spanning from 30.6 GHz to 37.12 GHz. The results showed improvement toward the target specifications yet required additional optimization steps.

#### IV. Final Optimized Design: Triangular Slot Integration

The triangular slot inside the triangular patch improved the geometry in the final design, as shown in Fig. 1(d), by providing an optimal ring thickness of  $b = 0.3$  mm. It improved the performance of the antenna. Eventually, this fourth model reached the desired resonance frequency of 34 GHz with a return loss of -29.82 dB and a bandwidth of 6 GHz that extended from 30.63 to 36.63 GHz, as shown in Fig. 2. This result met the goals; thus, the modifications in this design were quite effective.

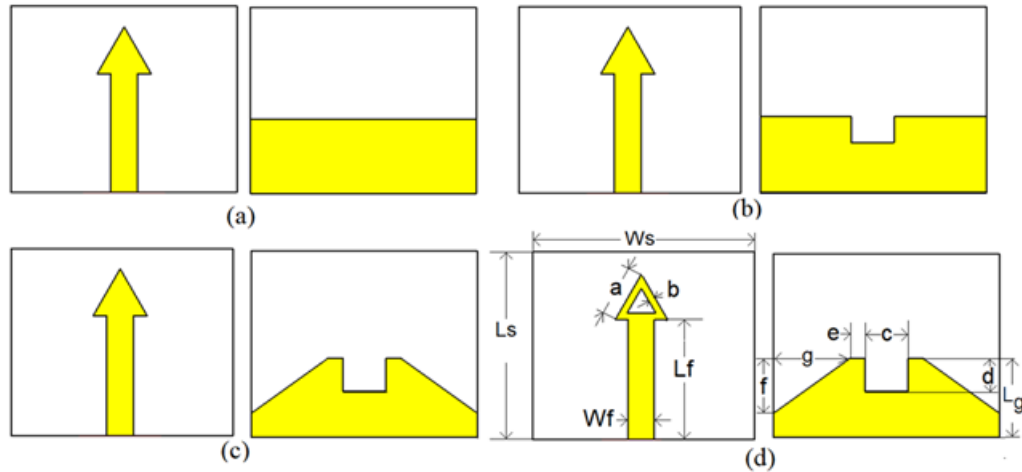


Fig. 1: Evolution of the proposed antenna design, showcasing both front and back views: (a) Initial Design, (b) Integration of Slots, (c) Addition of Triangular Cuts, and (d) Final Design with Triangular Slot Integration.

##### 1.1. Overview of Results

This sub-section initiates with Fig. 2, showing the simulated return loss across the iterative design stages of the proposed 34 GHz arrow-shaped microstrip antenna for 5G applications. From the starting geometry represented in red, with a uniform partial ground plane and a triangular patch, the desired resonance was not obtained, reflecting poor impedance matching. As expected, this resulted in suboptimal performance of the designed antenna. Introduction of a rectangular slot in the partial ground plane, represented in blue, improved impedance matching by yielding a resonant frequency of 37.4 GHz at -26.5 dB return loss. However, this iteration has deviated from the target frequency. Further refinements reduced the resonant frequency to 34.25 GHz at -24.44 dB return loss, incorporating triangular cuts in the ground plane. Lastly, integrating a triangular slot with another triangular slot inside the patch resulted in achieving the required operating frequency of 34 GHz, with an enhanced return loss of -29.82 dB and bandwidth of 6 GHz (from 30.6 to 36.6 GHz). This shows that the optimizations done on the structure are crucial

to meeting the very stringent performance requirements of 5G applications and underlines the effectiveness of the design methodology in effectively trading off compactness against bandwidth and gain.

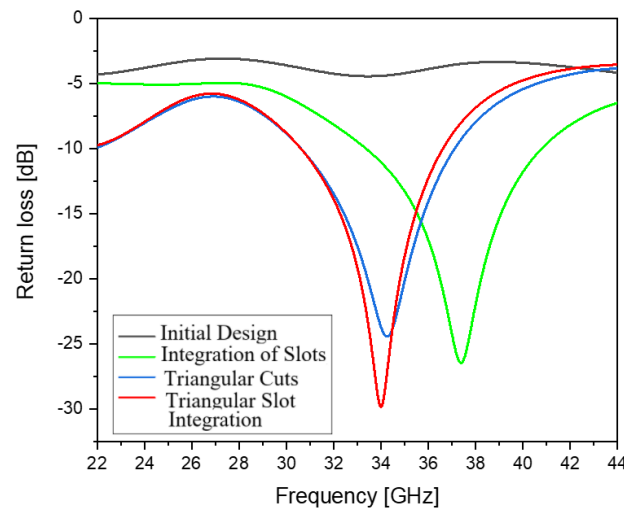


Fig. 2: Comparison of Return Loss Across Antenna Design Iterations.

To determine the optimal substrate dimensions, hundreds of different configurations were investigated. The best results, as demonstrated in Figures 3 and 4 and listed in Table 2, were achieved with a substrate dimension of  $10.2 \times 11.8 \text{ mm}^2$ . This configuration yielded a return loss of -29.82 dB at the operating frequency of 34 GHz, with a bandwidth of 6 GHz. The smallest return loss, -67.2 dB, was achieved for a resonant frequency of 33.725 GHz, while the bandwidth for this case has been 6.1 GHz. Fig. 3 presents the simulated return loss for different substrate dimensions at the resonant frequency of 34 GHz. It shows how vital substrate dimensions are to get the best result from the antenna. Amongst them, the substrate dimension of  $10.2 \times 11.8 \text{ mm}^2$  has given a return loss of 29.82 dB with a bandwidth of 6 GHz. This will provide a structure that will satisfy the aim of the design: minimum return loss and wide operational bandwidth. The data underline the importance of fine-tuning the physical dimensions in order to improve electromagnetic compatibility and performance at the frequency of interest. Large variations in return loss value versus substrate dimensions prove high sensitivity of impedance matching and resonant behavior of antenna to structural parameters.

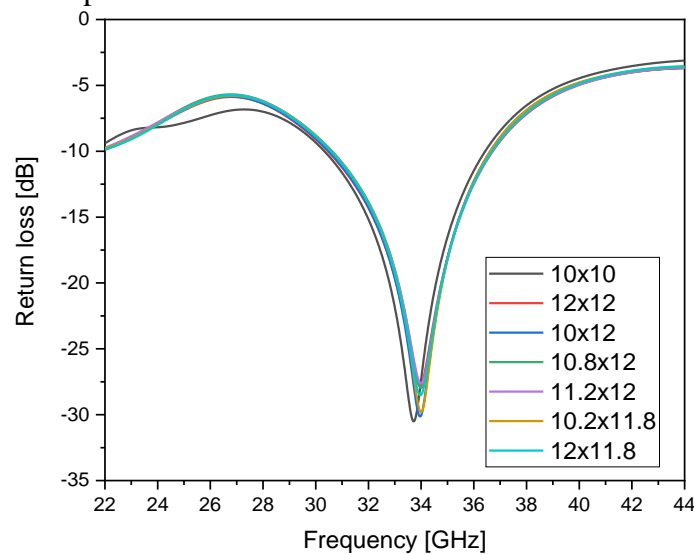




Fig. 3: Simulated Return Loss for Various Substrate Dimensions at 34 GHz Resonant Frequency

Fig. 4 gives the simulated return loss for different substrate dimensions when the resonant frequency is slightly shifted at 33.725 GHz. It can be noted that, for a substrate size of  $10.6 \times 10.4 \text{ mm}^2$ , the minimum value of return loss has reached -67.2 dB with an equivalent bandwidth of 6.1 GHz. That result indicates another possibility with a better impedance matching but on a shifted resonant frequency. The graph illustrates the trade-offs in antenna design: extreme values of return loss may require some compromise in the exact operational frequency. This type of information is very valuable in situations where the requirement for small signal reflection is more important than adherence to a specific frequency.

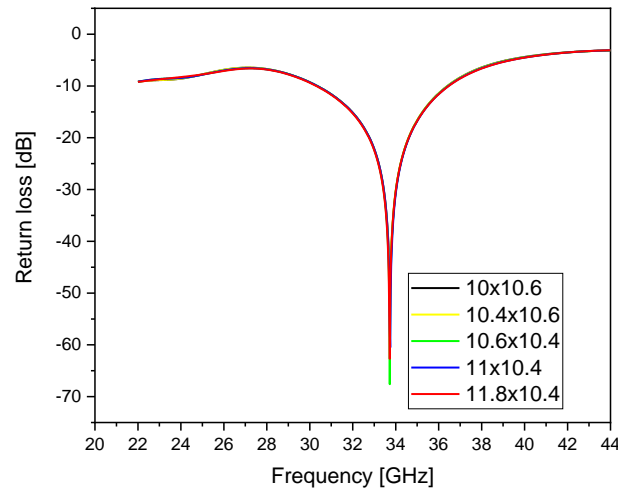


Fig. 4: Simulated Return Loss for Various Substrate Dimensions at 33.725 GHz Resonant Frequency

Table 2 presents the proposed 34 GHz arrow-shaped microstrip antenna with some antenna designs developed so far for 5G applications. A comparison is drawn based on dimensions, operating frequency ranges, resonant frequency, gain, and bandwidth. It is observed that the proposed antenna has better performance metrics as associated with antennas. The comparison reveals that the proposed antenna design strikes a balance among compactness, wide bandwidth, and steady gain, unlike several other designs reported for similar frequency bands.

Table 2: Comparison of Antenna Substrate Dimensions for Resonant Frequencies 33.72 GHz and 34 GHz

Sub. Dim. $\text{mm}^2$	Resonant [GHz]	Return Loss [dB]	BW [GHz]
10 × 10.6	33.725	-44.9	30.3-36.5
10.4 × 10.6	33.725	-45	30.3-36.4
10.6 × 10.4	33.725	-67.2	30.3-36.4
11 × 10.4	33.75	-60.4	30.33-36.5
11.8 × 10.4	33.725	-62.5	30.3-36.5
10 × 10	33.72	-30.5	30.33-36.4
12 × 12	33.95	-27.79	30.45-36.7
10 × 12	33.96	-30.14	30.49-36.6
10.8 × 12	34	-28	30.64-36.66
11.2 × 12	34	-27.6	30.6-36.7
10.2 × 11.8	34	-29.8	30.6-36.6

12×11.8	34	-28.5	30.6-36.6
---------	----	-------	-----------

Table 2 depicts a comparison of different designs and the superior performance of the proposed antenna for the maximum gain and bandwidth, which are 4.2 dB and 6 GHz, respectively, over a very compact area of  $10.2 \times 11.8 \text{ mm}^2$ . The result of this analysis confirms that it has excellent practicality with respect to 5G applications tending towards large requirements like higher data rates and low-latency communication. This balance between the performance and the capability of integration shows the potentials of the proposed antenna to cater to the demand of next-generation wireless networks. The return loss, resonant frequency, and operating bandwidth for the optimum substrate dimensions are shown in Figs. 5 and 6. In particular, the resonant frequency corresponding to the substrate dimensions of  $10.2 \times 11.8 \text{ mm}^2$  is 34 GHz and that corresponding to  $10.6 \times 10.4 \text{ mm}^2$  is 33.725 GHz. Fig. 5 presents the simulated return loss of the proposed design at an operational frequency of 34 GHz. The optimization of a return loss as good as -29.82 dB and the reflection of a very small amount of signal evidence excellent impedance matching. Further, the operating bandwidth ranges from 30.6 GHz to 36.6 GHz, indicating stable antenna performance over a wide frequency range. This return loss ensures that the signal has efficient transmission, and thus, the antenna is highly suitable for high-speed and reliable 5G communication systems.

By comparison, Fig. 6 presents the simulated return loss for the proposed antenna design on an alternative substrate dimension that resonates at 33.725 GHz. The magnitude of return loss at this frequency is as low as -67.2 dB, which shows very good impedance matching. The bandwidth achieved is from 30.3 GHz to 36.4 GHz, comparable to the optimal design. This represents, however, a compromise: the very low return loss has been bought at the expense of a small deviation from the frequency to be targeted. This realization could be of great consideration in applications where signal reflection, rather than adhering strictly to a specific resonant frequency, is of primary importance.

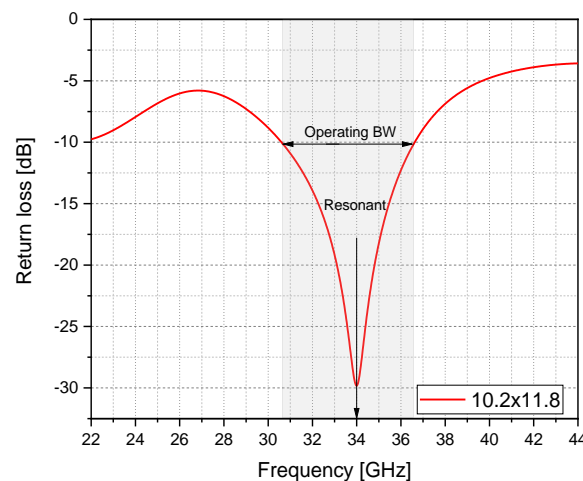


Fig. 5: Simulated Return Loss for the Proposed Antenna at 34 GHz Operating Frequency

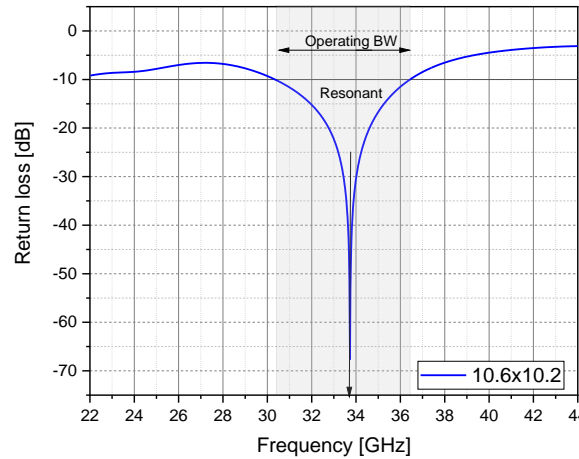


Fig. 6: Simulated Return Loss for the Proposed Antenna at 33.725 GHz Operating Frequency

Fig. 7 shows the simulated gain over frequency for two substrate dimensions:  $10.2 \times 11.8 \text{ mm}^2$  and  $10.6 \times 10.4 \text{ mm}^2$ . The optimal substrate dimension in terms of gain is  $10.2 \times 11.8 \text{ mm}^2$ , whose gain curve peaks at 4.2 dB at 34 GHz, while that of the other configuration peaks at 4.17 dB. It reveals that the main role of precision in the dimension selection is about enhancing some antenna performance metrics. Besides, the higher gain from the  $10.2 \times 11.8 \text{ mm}^2$  substrate dimension shows it is suitable for 5G applications because the signal strength is assured to be good and properly transmitted. The following section will summarize the two dimensions for substrates to finalize the analysis. Fig. 7 shows the best substrate dimension of  $10.2 \times 11.8 \text{ mm}^2$  showed higher gain at 34 GHz in every run, which proves it is the best configuration.

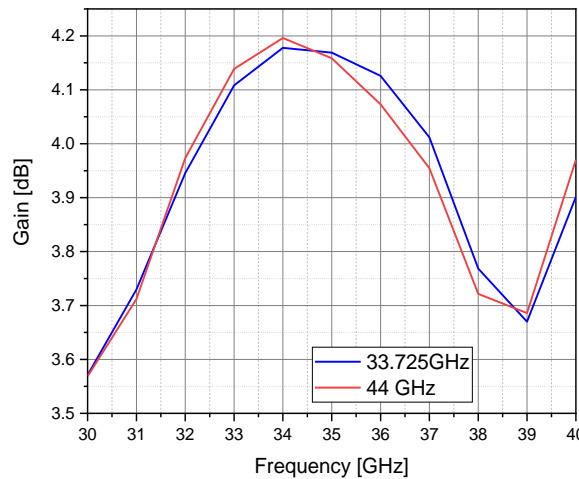


Fig. 7: Simulated Gain Across Frequencies for Substrates  $10.2 \times 11.8 \text{ mm}^2$  and  $10.6 \times 10.4 \text{ mm}^2$

Fig. 8 shows the simulated two-dimensional radiation patterns of the proposed antenna at three frequency points: 32 GHz, 34 GHz, and 36 GHz. All the patterns are basically directional with a maximum energy in one direction, especially around the resonant frequency at 34 GHz. Moreover, the slight variations observed in the patterns at 32 GHz and 36 GHz highlight the antenna's consistent performance across its operating bandwidth. This directional behavior is a crucial feature for targeted signal delivery in 5G networks, as it significantly enhances communication efficiency while minimizing interference. It is worth noting that the radiation pattern serves as the final parameter of this investigation. Specifically, Fig. 8 showcases the 2D radiation patterns for the operating bandwidth frequencies, including the resonance frequency of 34 GHz. Across the analyzed

frequencies, the radiation patterns exhibit a somewhat directional nature, further validating the antenna's effectiveness.

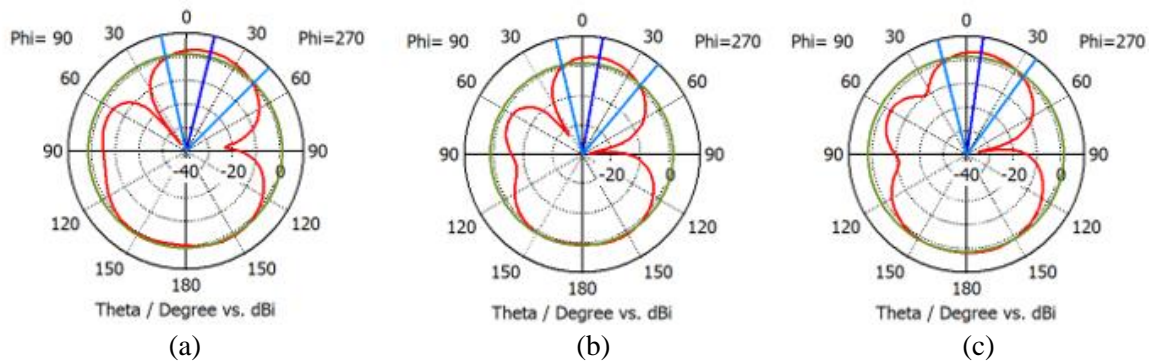


Fig. 8: Simulated 2D Radiation Patterns at Frequencies (a) 32 GHz, (b) 34 GHz, and (c) 36 GHz

A detailed comparison between the proposed antenna and that obtained from a few of the previously reported papers in the available literature related to 5G applications can be shown in Table 3. For this, many beneficial radiation features were exhibited through the proposed antenna: comparable bandwidth to or sometimes superior than several earlier reported; besides, broad bandwidth agreed well in most of the available works reporting performance capability in both cases. These attributes strongly support the suitability of the proposed design for implementation in 34 GHz resonant communication systems.

Table 2: Comparison of the Proposed Antenna with Results from Previous Studies

Ref.	Dimension mm <sup>2</sup>	Operational band [GHz]	Resonance Frequency [GHz]	Gain [dB]	BW
[9]	Single 6.2×8.4	25.3–32	28.5	7.4	6.7
	Mirrored 16.6×16.6	24.24 - 32	28.5	8.014	6.6
	Looped 18.8×14.4	24.2 - 30.8	28.5	7.62	7.74
	18.8×28.8	24.35–31.7	28.5	8.29	7.35
[12]	33×29	4.03-6.32	6	4.1-4.75	2.3
[13]	14×12	26.65-29.2 36.95-39.05	28/38	1.27,129	2.55,2.1
[14]	4×6	-	38/60	6.5.6.2	2,3.2
[15]	11.5×8.5	2.8-3.81	3.47	4.01	1.1
[16]	8.4×8.4	32.16-37.5	33.83/35.5	5.34	3.72
[17]	7×7	16.84-18.15 24.78-27.4 34.47/37.22 3.2-3.83	17.39/25.98/3 5.83	5.32	1.31/2.64/2.73
[18]	32×32	4.65-4.76 6.16-6.46	3.72	2.5	0.1/0.1/0.3
[19]	40×40	2.67-4.2	3.29	3.92	1.53
[20]	46×46	2.44-2.54 3.19-3.55	2.4	4	0.1/0.36
[21]	40×30	3.3-4	3.65	2.5	0.7
[22]	78×58	3.89-5.9	4.28	3	2.01

[23]	36×36	2.8-3.81	3.47	4.08	1.01
proposed	10.4×11.8	30.6-36.6	34	4.2	6

Table 3 compares the proposed antenna with some of the previous works that have been focused on 5G applications. This is analyzed by taking critical parameters into consideration: antenna dimensions, operating frequency bands, resonant frequencies, gain, and bandwidth as follows:

1. The proposed antenna has compact dimensions of  $10.4 \times 11.8 \text{ mm}^2$ , hence it is suitable for integration into modern 5G devices. This size is significantly smaller than most designs reviewed, which range up to  $78 \times 58 \text{ mm}^2$ , emphasizing the compactness of the proposed design without compromising performance.

2. The proposed antenna achieves an operational bandwidth of 6 GHz (30.6–36.6 GHz). This broad bandwidth is comparable to or superior to prior designs, ensuring effective coverage for 5G frequency bands. For instance:

- Ref. [9] reports a bandwidth of 6.7 GHz within a lower frequency range (25.3–32 GHz).
- Ref. [16] achieves a similar bandwidth of 5.34 GHz but within a narrower range (32.16–37.5 GHz).

3. The antenna is precisely tuned to resonate at 34 GHz, aligning with the target frequency for high-speed 5G communications. Many prior works target different bands, such as:

- Ref. [12]: Resonates at 6 GHz.
- Ref. [14]: Dual resonance at 38 GHz and 60 GHz.

This highlights the specific design focus of the proposed antenna for the 34 GHz band, catering to a niche yet critical application area within the 5G spectrum.

4. It realizes a gain of 4.2 dB, relatively moderate against some other works, such as Ref. [9], which achieves 7.4 dB; the proposed design strives to balance compactness with performance. This is quite good enough to ensure reliable communications in 5G networks, especially when combined with the directional pattern of radiation.

5. Among the advantages brought in by a proposed antenna are compact dimensions, which allow for easy integration into portable and space-constrained devices, hence guaranteeing flexibility in the design of modern 5G systems. Besides, it enables effective communication over a wide frequency range, increasing the overall reliability and adaptability within 5G networks. The antenna also ensures consistent performance, maintaining signal strength for efficient high-quality wireless communication in next-generation applications.

6. The proposed antenna is compact in size, has broad bandwidth, and directional radiation characteristics, which makes it highly suitable for wide bandwidth utilization to achieve fast data rates with minimum delays in 5G systems that support stable connections in densely populated urban areas.

These performances of full integration shown in Table 3 ensure the practicality of the proposed antenna for resonant communication systems at 34 GHz, hence offering potential for addressing the challenges of next-generation wireless networks, establishing its potential to address the challenges of next-generation wireless networks effectively. To this end, the design of an artificial printed multiband antenna for 5G, as in [24], is done.

## 4 Conclusion

The proposed arrow-shaped microstrip antenna with a triangular slot has excellent

performance for the 34 GHz 5G frequency band. By using a very simple arrow-shaped patch and a partial ground plane, the antenna exhibits a gain of 4.2 dB, a wide bandwidth of 6 GHz (30.6–36.6 GHz), and a return loss of  $-29.82$  dB for efficient impedance matching and low signal reflection. Fabricated on a Rogers RT/Duroid 5880 substrate of dimensions  $10.6 \times 11.8 \times 0.254$  mm<sup>3</sup>, it keeps a compact and lightweight form for being integrated into modern mobile and base station devices. Its directional radiation pattern ensures that the energy is concentrated in the target direction, reducing interference and further improving communication efficiency. By going through several iterations in design optimization, including the introduction of a triangular slot and the modification of the partial ground plane, poor impedance matching and narrow bandwidth problems have been overcome. Consequently, the resultant antenna realizes stable gain, broad bandwidth, and high power transfer, superior to many previous designs. The compact structure, low profile, and reliable performance of the antenna make it practical and efficient for millimeter-wave 5G systems to enable high-speed data transmission, low latency in communication, and enhanced broadband performance in next-generation wireless networks.

### Funding

This project received no funding.

### Conflict of Interest

The authors declare no conflict of interest.

### Data Availability

The datasets analyzed during this study are available from the corresponding author upon reasonable request.

## References

- [1] J. Guo, C. A. Guo, M. Li, & M. Latva-aho. (2025). Antenna technologies for 6G – advances and challenges. *IEEE Transactions on Antennas and Propagation*.
- [2] P. K. Sharma, V. P. Yadav, A. N. Mukesh, S. Jawale, & A. Kumar. (2024). Optimizing antenna design for 6G applications using machine learning techniques. *Proceedings of the 2024 International Conference on Artificial Intelligence and Emerging Technology (Global AI Summit)*, (700–704). IEEE.
- [3] R. Kumar, A. Chandra, V. K. Vytla, & M. R. Sodam. (2023). A flexible microstrip antenna for wireless communication applications. *Proceedings of the 2023 International Conference on Next Generation Electronics (NEleX)*, (1–4). IEEE.
- [4] S. Thirugnanasambandam & I. Govindanarayanan. (2023). Wideband tripolarized circular patch antenna for fifth-generation access point applications. *AEU – International Journal of Electronics and Communications*, 170.
- [5] S. Kundu & A. Chatterjee. (2022). A compact super wideband antenna with stable and improved radiation using super wideband frequency selective surface. *AEU – International Journal of Electronics and Communications*, 150, 154200.

- [6] E. Joseph, P. Kumar, & T. J. O. Afullo. (2023). Design and performance analysis of a miniaturized circular arc slotted patch antenna for ultra-wideband applications. *Proceedings of the 2023 International Conference on Electrical, Computer and Energy Technologies (ICECET)*, (1–5). IEEE.
- [7] J. S. Alkasassbeh, A. Y. Hindi, I. Trrad, M. O. Dwairi, E. A. Dwairi, & M. Alja'fari. (2025). Design and optimization of a compact inset feed microstrip antenna for 5G applications with enhanced MIMO performance. *Engineering, Technology & Applied Science Research*, 15(2), 21373–21382.
- [8] M. O. Dwairi. (2021). Increasing gain evaluation of 2×1 and 2×2 MIMO microstrip antennas. *Engineering, Technology & Applied Science Research*, 11(5), 7531–7535.
- [9] S. I. Farghaly, K. E. Abo Al-Ela, A. Y. Zaki, et al. (2025). New design of microstrip patch antenna at 28 GHz and MIMO configuration with improved characteristics for IoT applications. *Journal of Wireless Communications and Networking*, 2025(59).
- [10] M. O. Dwairi, M. S. Soliman, A. Y. Hendi, & Z. Al-Qadi. (2023). The effect of changing the formation of multiple-input multiple-output antennas on the gain. *International Journal of Electrical and Computer Engineering*, 13(1), 531–548.
- [11] B. G. P. Shariff, et al. (2025). High-gain narrow-beam MIMO array antenna operating at n260 band for millimeter wave applications. *IEEE Access*, 13, 69395–69412.
- [12] I. Shaik & S. K. Veni. (2023). A novel quadrangular slotted DGS with a wideband monopole radiator for fifth-generation sub-6 GHz mid-band applications. *Progress in Electromagnetics Research C*, 133, 109–120.
- [13] Md. N. Hasan, S. Bashir, & S. Chu. (2019). Dual-band omnidirectional millimeter wave antenna for 5G communications. *Journal of Electromagnetic Waves and Applications*, 33(12), 1581–1590.
- [14] M. H. Sharaf, A. I. Zaki, R. K. Hamad, & M. M. M. Omar. (2020). A novel dual-band (38/60 GHz) patch antenna for 5G mobile handsets. *Sensors*, 20(9), 2541.
- [15] R. Swetha & A. Lokam. (2021). Novel design and characterization of wideband hook-shaped aperture coupled circularly polarized antenna for 5G application. *Progress in Electromagnetics Research C*, 113, 161–175.
- [16] J. Muralidharan. (2020). Wideband patch antenna for military applications. *NJAP*, 2(1), 25–30.
- [17] C. L. Bamy & P. Moukala Mpele. (2022). Asymmetric-fed triband antenna for military radars and 5G applications using microstrip technology. *Journal of Engineering*, 739–745.
- [18] R. Krishnamoorthy, A. Desai, R. Patel, & A. Grover. (2021). 4-element

- compact triple band MIMO antenna for sub-6 GHz 5G wireless applications. *Wireless Networks*, 27(6), 3747–3759.
- [19] L. C. Paul, H. K. Saha, T. Rani, et al. (2022). An omni-directional wideband patch antenna with parasitic elements for sub-6 GHz band applications. *International Journal of Antennas and Propagation*, 2022, 1–11.
- [20] S. Nelaturi. (2021). ENGTL-based antenna for Wi-Fi and 5G. *Analog Integrated Circuits and Signal Processing*, 107(1), 165–170.
- [21] A. Kapoor, R. Mishra, & P. Kumar. (2020). Compact wideband-printed antenna for sub-6 GHz fifth-generation applications. *International Journal on Smart Sensing and Intelligent Systems*, 13(1).
- [22] Desai, T. Upadhyaya, J. Patel, R. Patel, & M. Palandoken. (2020). Flexible CPW fed transparent antenna for WLAN and sub-6 GHz 5G applications. *Microwave and Optical Technology Letters*, 62(5), 2090–2103.
- [23] R. Wu & C. Hu. (2021). Elliptical slot microstrip patch antenna design based on a dynamic constrained multiobjective optimization evolutionary algorithm. *International Journal of Cognitive Informatics and Natural Intelligence*, 15(4).
- [24] S. Palanisamy, G. M. Abdulsahib, O. I. Khalaf, A. S. S., W.-K. Wong, & S.-H. Pan. (2023). Design of artificial magnetic conductor-based stepped V-shaped printed multiband antenna for wireless applications. *International Journal of Advanced Soft Computing and Applications*, 15(3).

### Notes on contributors



**Jawdat S. Alkasassbeh** (Senior Member, IEEE) was born in Jordan in 1983. He received a B.Sc. degree in communications engineering from the Department of Electrical Engineering, Faculty of Engineering, Mutah University, Al-Karak, Jordan, in 2006, and a master's degree in communications engineering from the University of Jordan, Amman, Jordan, in 2011. He received a PhD degree from the School of Mechanical Engineering and Electronic Information, China University of Geosciences, Wuhan, China, in 2021. His current research interests include applications of evolutionary algorithms, applied AI, power reduction of mobile communication mechanisms, digital wireless communication systems, radio link design, image processing, UWB microstrip patch antennas, and dielectric resonant antennas. He can be contacted at: jawdat1983@bau.edu.jo.





**Farouq Mohammad Al-Taweel** is an Associate Professor at Al-Balqa Applied University, specializing in communication engineering with a focus on multi-communication channel characteristics. His research interests include the analysis and design of satellite communication systems and security. Dr. Al-Taweel received his Ph.D. in Electrical Engineering/Communication from Moscow Technical University of Communications and Informatics in 1993 and his Master's degree in Electrical Engineering (Communication) from Leningrad State University in 1989. He can be contacted at: [dr\\_farouq@bau.edu.jo](mailto:dr_farouq@bau.edu.jo)



**Majed O. Dwairi** (Member, IEEE) is a Full Professor in the Department of Electrical Engineering, Faculty of Engineering Technology, Al-Balqa Applied University, Amman, Jordan. His research interests include optical and wireless communications, signal and image processing, UWB microstrip patch antennas, dielectric resonator antennas, antenna measurement techniques, and optimization methods in antenna design. Dr. Dwairi is a member of IEEE and IEEE AESS. He can be contacted at: [majeddw@bau.edu.jo](mailto:majeddw@bau.edu.jo)



**Aws Al-Qaisi** is a Professor in the Department of Electrical Engineering, College of Engineering and Technology, American University of the Middle East, Kuwait. He received his Ph.D. (2006) and M.Sc. (2010) in Communication and Signal Processing from Newcastle University, UK. Prof. Al-Qaisi is a member of the IEEE Executive Committee in Jordan, responsible for the industrial section. His research interests include feature extraction, artificial intelligence algorithms and transformations, and digital communication. He has served as a reviewer for numerous international journals and has published over 31 scientific papers in communication and signal processing.



**Maen Takturi** is a professor of electrical engineering at the American University of the Middle East (AUM). He holds a B.Sc. and M.Sc. in electrical engineering from the University of Jordan and obtained his Ph.D. in electrical engineering from the University of Technology, Sydney (UTS), Australia, in 2010. Prof. Takturi served as a Visiting Researcher in the Department of Electrical and Electronic Engineering at the University of Melbourne. During his tenure at UTS, he was an active member of the Centre for Real-Time Information Networks (CRIN). Subsequently, he joined the American University of Ras Al Khaimah (AURAK), UAE, where he held several academic and leadership roles, including Chairman of the Department of Electrical, Electronics, and Communications Engineering, Director of Research at the School of Engineering and Computing, and Director of the Advanced Technology and Artificial Intelligence Center. His research interests include artificial intelligence, signal processing and data fusion, estimation theory, target tracking, biomedical systems, renewable energy, machine learning, image processing, and the Internet of Things. He can be contacted at: [maen.takturi@aum.edu.kw](mailto:maen.takturi@aum.edu.kw)